Journal of Ship Research, Vol. 48, No. 2, September 2004, pp. xx–xx

High-Speed Trimaran Drag: Numerical Analysis and Model Tests

Igor Mizine,[*] **Eduard Amromin,**[†] **Leonard Crook,**[‡] **William Day,**[‡] and **Richard Korpus§**

[*]*Science Applications International Corporation, USA*
[†]*Mechmath LLC, Prior Lake, Minnesota, USA*
[‡]*David Taylor Model Basin, Carderock Division, NSWC, USA*
[§]*Applied Fluid Technologies, Inc., Annapolis, Maryland, USA*
Manuscript received at SNAME headquarters January 22, 2002; revised manuscript received August 20, 2003.

AU1

A numerical technique for high-speed trimaran resistance calculation is developed. The technique is based on the modified viscous-inviscid interaction concept and quasi-linear theory of wave resistance (Amromin et al 1984). The key element of this technique, which is called modified quasi-linear theory (MQLT), is an account of Froude number influence on the ship trim, transom drag, and wetted surface. This influence leads to appearance of a drag component that significantly depends on both Reynolds number and Froude number. This component has been traditionally included in residuary drag in the model test data. The presented preliminary numerical results were obtained with simplifications of the boundary layer theory that are acceptable for slender hulls. Calculated drag is in sufficient accordance with results of model tests. The MQLT computations of boundary layers are also compared with the Reynolds averaged Navier-Stokes (RANS) calculations (one-equation turbulence model by Spalart and Allmaras 1992) at model and ship scale Reynolds numbers. An analysis of the model–ship scale correlation factor for high-speed slender hulls with transom sterns and diverse mutual position of the trimaran hulls is done.

Introduction

EXISTING AND FORTHCOMING markets demand large high-speed ships with wide decks for high-speed sea transportation of a large amount of high-valued and relatively light cargo (Kennel 1998). A trimaran configured from slender hulls (Avis et al 1999, Mizine & Amromin 1999) is among the best design concepts.

For any high-speed ship, hydrodynamic drag is a key problem of design. Theoretically, an appropriate mutual location of trimaran hulls can significantly reduce wave resistance for a narrow range of Froude numbers. Practically, numerous design restrictions limit longitudinal and transverse distances between the side hulls and the center hull.

Trimaran configurations of minimal wave resistance can be predicted by using contemporary computer fluid dynamic (CFD) codes. Computations of wave resistance (Mizine & Amromin 1999, Yang et al 2000) can be provided for a range of trimaran configuration parameters. Such predictions are in satisfactory agreement with measurement of residuary drag during towing tests. However, for high-speed slender-hull trimarans with transom sterns, configurations of minimal predicted wave resistance do not necessarily coincide with configurations of minimal measured residuary drag.

In any minimization of ship wave resistance, an attainable reduction of wave resistance must be compared with a possible attendant increase of other drag components. There has been significant progress in estimations of these components for conventional ships (Karafiath 1997, Larsson et al 1998). For ships with relatively new hull forms, and nonconventional high-speed speed range, the unexpected ratios of drag component are encountered because of physical flow characteristics. The reported experiments manifest that for a high-speed trimaran, the trim is the key drag-affecting characteristic. A significant running trim affects the trimaran drag in three main ways. First, the trim changes the shape of a submerged part of hulls, and that affects the wave resistance. Second, the trim changes submergence of the transom, and this affects the form resistance. Third, the trim changes the wetted surface, and that affects the frictional resistance.

The issue is that it is impossible to separate viscous and inviscid effects there because the trim depends on both Froude number and Reynolds number (Orihara & Miyata 2000). A theoretical/numerical analysis of viscous-inviscid interaction for a large high-speed

trimaran in the range of Froude numbers $0.3 < \mathrm{Fn} < 0.6$ is necessary for both optimum trimaran hull design and a realistic extrapolation of the model test results to full-scale conditions. Further, because of the necessity to provide a multivariant optimization in the course of the trimaran design, it is reasonable to use relatively simple theoretical/numerical methods, such as modified quasi-linear theory (MQLT). Such a method and the results of validation by comparison with both Reynolds averaged Navier-Stokes (RANS) code results and the model test results provided in the David Taylor Model Basin (DTMB) are described in this paper.

Quasi-linear theory of ship wave resistance

The first step in estimating the residuary drag is computation of wave resistance of trimaran with the fixed draft and trim. According to the conventional ideas, ship wave resistance does not depend on Rn value and can be calculated using the following problem for the velocity potential ϕ:

$$\Delta\Phi = 0 \tag{1}$$

$$(\nabla\Phi, N)/_{S+S^*} = 0 \tag{2}$$

$$(\nabla\Phi, T)/_{S^*} = V_S(1 - gY/Vs^2)^{0.5} \tag{3}$$

$$\nabla\Phi(x \to -\infty) = \{V_S, 0, 0) \tag{4}$$

Here N is the unity normal to the free surface S^* or hull surface S, and T is the unity tangent to the streamlines on these surfaces.

The problem (1) to (4) is a three-dimensional, nonlinear problem. Because of the computational difficulty of solving such a problem, there were numerous attempts to solve a similar problem within the framework of linear theory that is correct for waves of very low amplitudes and hulls of very high slenderness. The relevant mathematical technique has been perfectly developed, and its application to routine engineering is of no problem. For real ships, this refined theory (Havelock 1934) usually gives overestimated wave amplitudes. This circumstance has urged development of numerical techniques to solve the nonsimplified problem (1) to (4). In spite of some successes (Ando et al 1990, Lalli et al 1992, Larsson et al 1998), the computational and mathematical difficulties still remain. Particularly, the computation results remarkably depend on meshes over S^* and S. Such a dependency is easily understandable: using any of the direct numerical techniques, the value of C_w, which is about 10^{-3} must be calculated as a sum of quantities, which values are about 10^{-1}. As a result, about 10^6 panels are necessary for such computations of a monohull wave resistance (Larsson et al 1998). Because of these issues, a nonlinear correction to linear theory is still very attractive for engineering purposes.

The idea of such a correction is old enough. Perhaps Inui (1957) was the first to implement this idea with some success. Contrary to attendant speculations about taking into account viscous effects in estimating the pure wave component of ship resistance, in fact, he has suggested regulating results of the wave interaction by artificially limiting rules that are not rules of linear theory. Nonlinear theory of water waves can be a more comprehensible basis of such limiting rules. These rules can grow from nonlinear theory either directly (Amromin et al 1983, 1984) with the use of two-dimensional solutions (Salvesen & von Kerzeck 1976), or implicitly AU2
(Amromin et al 1993). To name this approach, the authors use a quasi-linear theory (QLT) method of wave resistance calculation.

QLT method is based on the calculation of the C_W using wave amplitude distribution far behind the ship (Havelock 1934); but density of wave energy Ψ is limited in QLT by an empirical constant denoted as E_M:

$$Cw = \left(\frac{g}{V_S{}^2}\right)^2 \frac{2L^4}{\pi S} \int_0^\infty \frac{\Psi(b)}{\sqrt{1+b^2}}\, db \tag{5}$$

Here $\Psi(b) = \min\{E_M, \Psi(b)\}$, $\beta = ikY_M\sin(\alpha)$, $\alpha = a\tan(b)$, b is the variable in integral (5). It runs across the ship's wake:

$$\Psi = \left|\frac{H(k,a)}{V_S L^2}\right|^2, \quad k = g\left(\frac{1+b^2}{V_S{}^2}\right),$$

$$H(k,a) = \sum_M \int_{X_{SM}}^{X_{RM}} \int_{-D_M}^{0} Q(x,z)\, e^{kz+\beta+ikx\cos a}\, dxdz,$$

Function $Q(x,z)$ can be taken from a linear theory. It is necessary to explain that the used value $E_M = 0.05$ is the certain effective maximum of the dimensionless density of the wave energy, and this maximum is not directly related to the energy of steady wave of maximum amplitude known as Stokes waves.

The function $Q(x,z)$ for a monohull ship certainly can be taken from a linear theory of the double hull, and even for multihull ships it can be usually done so, because a distance between its hulls is comparable with the hull length. For any given $Q(x,z)$, computation of the improper integral in (5) can be performed with the ordered accuracy by standard computational tools.

Corrections made in the formula (5) are more significant for low values of Fn, as one can understand from an example given in Fig. 1. It is seen that this rule for Ψ neither makes computational F1

Nomenclature

Fn = Froude number
Rn = Reynolds number
Φ = velocity potential
$N = \{N_x, N_y, N_z\}$ = normal to a boundary
S^* = water free surface
S = wetted surface area
S_T = transom area
D = ship's displacement
C_R = residuary drag coefficient
C_F = friction drag coefficient
C_W = wave resistance coefficient
C_T = transom drag coefficient
E_M = maximal wave energy density
L = ship total length
V_S = ship speed
Dm = draft hull (m)
Lm = length of hull (m)
Bm = beam of hull (m)
Sm = wetted surface area of hull (m)
X_{Tm} = transom abscissas of hull (m)
Ym = distance between center planes of center hull and side hull (m)
Q = intensity of equivalent hydrodynamic sources
$Y(x,z)$ = hull ordinates
δ = boundary layer thickness
δ^* = displacement thickness
δ^{**} = momentum thickness
$\theta, \theta^*, \theta^{**}$ = parameters in three-dimensional axisymmetric flow calculations
U = velocity on inviscid flow boundary
R = boundary radius in an auxiliary axisymmetric flow
τ_W = wall friction
R_W = body radius
Cp = pressure coefficient
C_{PT} = base pressure coefficient past the transom

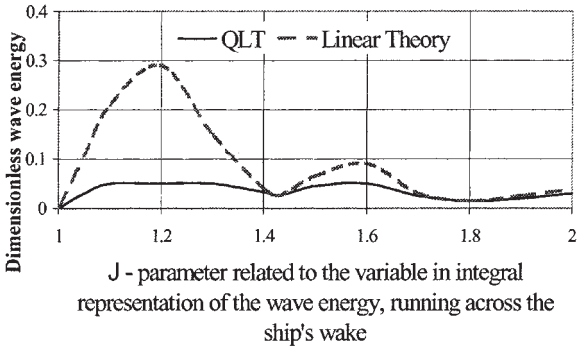

Fig. 1 Comparison of typical energy distributions behind a ship of moderate fullness in linear and non-linear theories as function of $J=1/\sim(1+b^2)$. QLT = quasi-linear theory

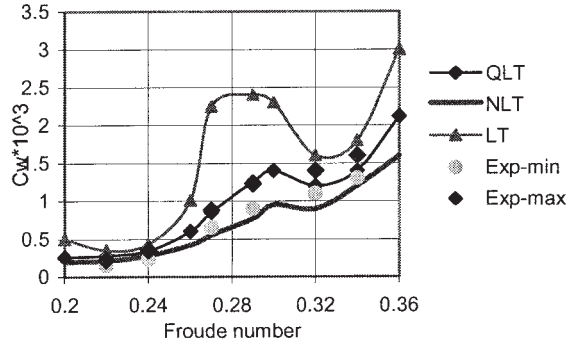

Fig. 2 Coefficient C_W of the model W4210 (Series 60). Linear theory results (LT) correspond to the Havelock formula. Nonlinear theory (NLT) results were obtained in Lalli et al (1992). Experimental data were presented in Ni et al (1989) with emphasis on maximal and minimal values. QLT = quasi-linear theory

difficulties, nor increases the computer time that is necessary for Michell formula (which can be deduced from the Havelock formula by substitution of the simplest Q).

An example of comparison of calculations with the formula (5) of QLT, classical linear theory, and a nonlinear numerical technique for the model W4210 from Todd's (1953) Systematic Serial of Models, Series 60 (with block coefficient 0.6), is shown in F2 Fig. 2. This figure also contains a generalization of relevant experimental data. For the aims of this study, the next comparison with experimental data should be done for a fast catamaran. There is F3 such a comparison in Fig. 3.

The difference in measured values of residuary drag coefficient in Fig. 2 is the difference between its mean values for the same model in different certified model tanks. It is below 0.0003 in this figure, but above 5% of maximal value of this coefficient in the presented Fn range.

As our long-term experience showed, QLT combines the advantages of linear theory (short time of computation and clear dependence of resistance on ship hull forms) and nonlinear theory (absence of oscillations of the function C_W [Fn] and its acceptable values in a wide range of Froude numbers).

Model tests results

After first application of QLT in a high-speed ship (and trimaran, particularly) design evaluation and hydrodynamic optimization (Mizine & Amromin 1999), it became necessary to validate the described method by comparing with the results of model tests. In December 1999 under Center for Commercial Deployment of Transportation Technologies (CCDOTT) funded project Kvaerner Masa Marine had provided hydrodynamic testing at the David Taylor Model Basin to determine resistance and seakeeping capability of high-speed trimaran models. A full-scale trimaran was designed with the center hull length of 313 m. Resistance tests with different side hull configurations at calm water and the sea state 5 and 7 tests were carried out with two models that have different shapes of the center hull stern. The model center hull length was 6.5 m.

The results of these model tests are described in Allison et al (2001) and Mizine and Thorpe (2000) and will be discussed below. Figure 4 from Mizine and Thorpe (2000) shows total resistance F4 curves for the two very high speed sealift trimaran (VHSST-50) variants with "aft" and "forward" position of the side hulls for calm

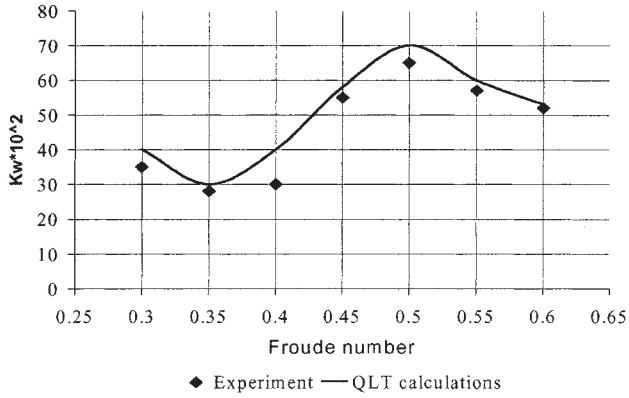

Fig. 3 Comparison of measured and computed coefficient $K_W = 2R_W/(\rho U_\infty^2 D^{2/3})$ for a catamaran (Huang & Cai 1991). QLT = quasi-linear theory

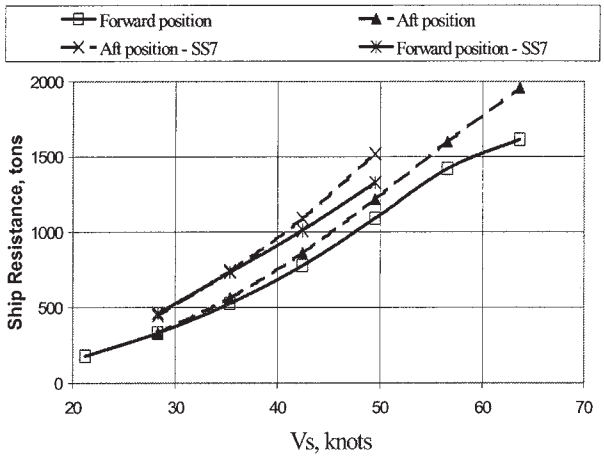

Fig. 4 Trimaran ship resistance. Extrapolation to full-scale data is made with towing tank results

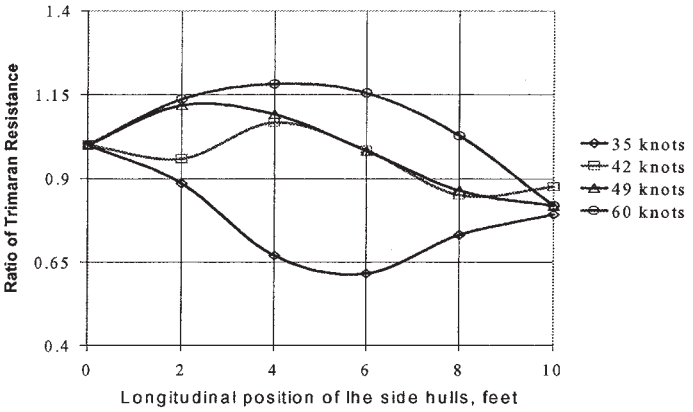

Fig. 5 Effect of side hull position ratio on measured resistance of Model B. Abscissa is the longitudinal positions of the side hull transoms forward the center hull transom (in feet). Ordinate is the ratio of trimaran resistance at different longitudinal position of the side hulls to trimaran resistance with the side hulls aft. Curve "35 knots" corresponds to full-scale speed of 35 knots, and so forth.

water and sea state 7 (significant wave height is 20 ft) based on the model test data. Figure 5 shows the effect of longitudinal spacing of the side hulls relative to the transom of the center hull.

The stern center hull forms of the initial Model A had a flat transom with the beam equal to the maximum beam of the center hull. Another variation of the stern hull forms was made to suit propulsion design sizing estimates and machinery arrangement of the "unified propulsion packages" (Allison et al 2001). Model B was built with an improved stern section.

Comparison of calculated wave resistance of the high-speed trimaran with measured residuary drag

The usual way to provide comparison with model test data is to calculate the sum of the wave resistance coefficient and the form resistance coefficient (named as residuary drag). The coefficient C_W relates to the gravity effect on the pressure distribution over the hulls. According to the common assumptions, C_w depends on Fn only. The form resistance appears due to viscous effects on pressure distribution on the hulls. According to the common assumption, which is used only to make the comparison of calculated and measured resistance, this component of drag is directly proportional to the friction and depends on Rn only. An individual proportionality coefficient was deduced from the model test results at low values of Fn. It is assumed that all features of the hull shapes (such as transom) are implicitly taken into account in this proportionality coefficient. The above-mentioned sum can then be calculated and compared with the measured data.

A towing procedure in the David Taylor Model Basin allows providing tests with both restricted and free trim. The first series of the towing tests with Model A was performed for restricted trim. For restricted trim, the DTMB standard technique to define the form resistance coefficient from the test data gave its value equal to 0.35. The comparison of computed and measured results for two diverse locations of side hulls of this model is plotted in Figs. 6 and 7. A similar comparison for one location of the side hulls relative to the center hull of the Model B is given in Fig. 8.

Discrepancies between calculated and measured data for different locations of side hulls, as well as for different models, can be found. Particularly, although the computations are in good correspondence with test data of the model with restricted pitch, there is no such correspondence for the free pitch and trim (see Fig. 8). This

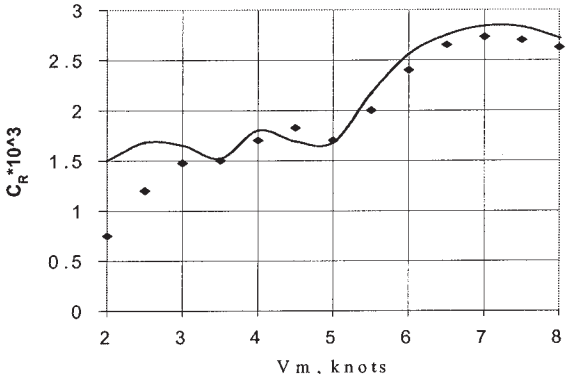

Fig. 6 Comparison of computed $C_R = C_W + 0.35\ C_F$ for the restricted trim (solid line) and measured C_R of the Model A in the aft position of the side hulls (squares)

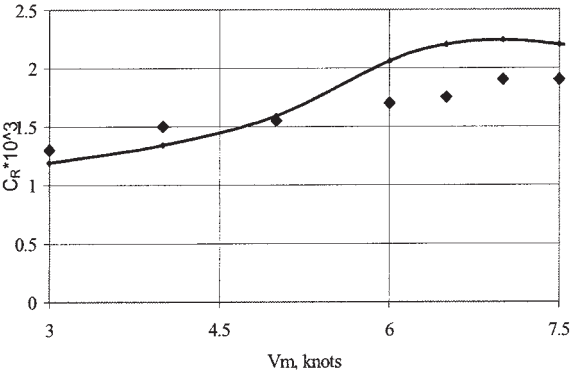

Fig. 7 Comparison of the calculated $C_R = C_W + 0.35\ C_F$ for the restricted trim (solid line) and measured C_R of the Model A in the forward position of the side hulls (squares)

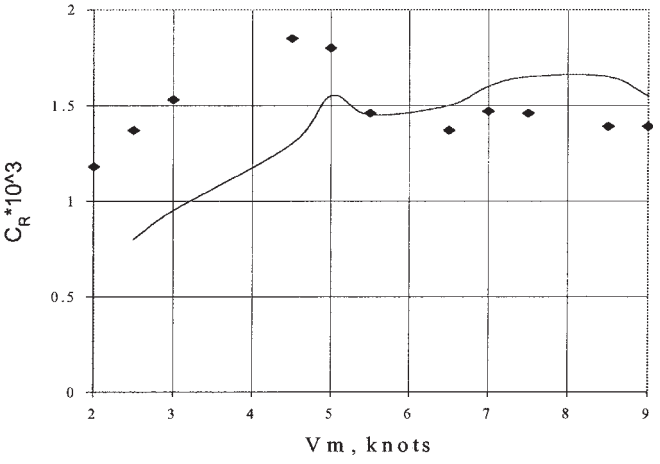

Fig. 8 Comparison of calculated $C_R = C_W + 0.35\ C_F$ (solid line) and measured C_R (squares) for the Model B

calculation overestimates the advantage of Model B relative to Model A with side hulls in the forward position at the speed of 7 m per second (which correspond to 50 knots ship speed). However, the advantage of the best variant of Model A is underestimated relative to its basic variant (which corresponds to the aft position of the side hulls). It is important to emphasize that the difference between computed and measured C_R has increased with the trim value.

As a result, the authors came to the conclusion that the conventional assumption about the Froude-independent form resistance coefficient does not work well for slender trimarans with transom sterns. First of all, trimaran running trim leads to high changes in the wetted surface and, consequently, in the ship friction, whereas the conventional procedure used for extracting drag coefficients from measured drag values adds the friction variations to C_R, because all coefficients are calculated for a Fn-independent wetted surface area. Determination of trim is a key step in prediction of the actual friction. Thus, introduction of the necessary correction to the residuary drag coefficient calculations requires solving a problem on the viscous-inviscid interaction.

Computation of trim

The trimaran sinkage and trim is a kind of two-dimensional motion of absolutely rigid body. Therefore, it is possible to describe this motion of three hulls by two variables that define a vertical position of the dynamic center of flotation and the ship trim. The coefficients A_1 and B_1 in the formula $dz = A_1 + B_1 x$ is used as such variables. These coefficients will be found from a pair of equations of the ship equilibrium under variations of hydrodynamic pressure and buoyancy, and under moments of these forces:

$$A_1 \sum_{m=1}^{3} \int_{X_{0m}}^{X_{0m}+L_m} Y(x,0)dx + B_1 \sum_{m=1}^{3} \int_{X_{0m}}^{X_{0m}+L_m} xY(x,0)dx = Fn^2 \sum_{m=1}^{3} \int_{S_{wm}} \delta C_P N_z dS \tag{6}$$

$$A_1 \sum_{m=1}^{3} \int_{X_{0m}}^{X_{0m}+L_m} xY(x,0)dx + B_1 \sum_{m=1}^{3} \int_{X_{0m}}^{X_{0m}+L_m} x^2 Y(x,0)dx = Fn^2 \sum_{m=1}^{3} \int_{S_{wm}} x\delta C_P N_z dS \tag{7}$$

Here is a difference of pressure coefficients for two vertical positions of the hulls at two close values of Fn. A necessity to consider this difference appears because equations (6) and (7) are written with the assumption about small variations of submerged volumes and pressure coefficients. Therefore, the values A_1 and B_1 must be determined by iterations for ~0.3–0.7. Then A_1 and B_1 give changes of trim at two successive Fn values: S_m implicitly depends on Fn and $Y(x,z)$ directly depends on Fn.

AU3 The custom path to find pressure distributions is to use the potential approach with the kinematic boundary condition (2), which can be rewritten as:

$$Q(x,z) - \frac{1}{2\pi} \sum_m \int_{S_m} \int Q(\xi, \eta) \frac{\partial}{\partial N} \frac{1}{R_{x\xi}} dS = -2N \tag{8}$$

Here $R_{X\xi}$ is the distance between a point of velocity calculation and the surfaces where the sources are distributed.

This well-known integral equation is written without an account of the free surface shape, and the Q distribution does not depend on Fn or wave shapes. The velocity in this flow can be calculated after determination of Q from equation (8).

The following formula is used for this calculation:

$$U(x,z) = \frac{1}{4\pi} \sum_m \int_{S_m} \int Q(\xi, \eta) grad \frac{1}{R_{x\xi}} dS + V_s \tag{9}$$

There are diverse possibilities to select the surfaces of integration in equations (8) and (9). The simplest possibility is to select hull center planes as S_m. As was shown, it is good enough for the computation of wave resistance, but computation of pressure requires distributing the sources over the body surfaces (Birkhoff & Sarantonello 1957).

The potential approach with the surface-distributed sources gives satisfactory values of C_P from the bow up to main part of the stern, and an unacceptable difference between numerical results and reality takes place on a small part of the stern only. Introduction of an effective frontier between viscous and inviscid parts of the flow is the well-known simplified method to estimate pressure in real fluid. Pressure distribution over such a frontier in ideal fluid practically coincides with pressure distribution over the hull in viscous fluid. A distance from this frontier to the hull surface equals the displacement thickness of the boundary layer. This concept of viscous-inviscid interaction is used below.

Modification of the QLT method: viscous-inviscid calculation of form resistance and transom drag

For slender hulls, a further significant simplification is acceptable due to the fact that the averaged (along cross-section) pressure distribution is close to the axisymmetric pressure distribution for a body of revolution of the same distribution of the cross-section areas. As was shown by Granville in 1974, the averaged boundary layer properties are also close enough, and the computed viscous part of the residuary drag is close to experimental data for such hulls (Amromin et al [1983] employed such bodies of revolution at smaller Fn and for transom-free hulls).

The characteristics of turbulent boundary layers undergo insignificant variations over the main part of the slender hull, and the high hull slenderness allows the next simplification of computations. It is acceptable for such hulls to fix the ratio $\delta^*/\delta^{**} = 9/7$ in Karman equation:

$$\frac{d\theta^{**}}{dx} + \frac{dU}{dx} \frac{\theta^{**}}{U} \left(2 + \frac{\theta^*}{\theta^{**}}\right) = \frac{\tau_W \tau_W}{\rho U^2} \tag{10}$$

This equation can then be rewritten in the following form:

$$\frac{d\delta}{dx} = \frac{36\chi[0.87 \log|xRn/(10^{0.325} L)|]^{-2.3} - \Omega}{7 + 4.2\sigma} \tag{11}$$

Here $\Omega = \frac{7}{r_W} \delta \frac{dr_W}{dx} + \frac{129 + 33\sigma}{5U} \delta \frac{dU}{dx}$, $\sigma = \delta/r_w$, χ is the ratio of the section length on the original hull to the half-circle length on the auxiliary body of revolution, and $\delta = 5.2\ (x\ L/Rn)^{1/}$ for $xRn/L < Rn^* \sim 10^6$. The corresponding formula for the dis- AU4
placement body radius over the hull is a following consequence of equation (11):

$$R(x) - r_w(x)[1 + 0.25\sigma(x) + 0.667\sigma\ (x)^2]^{1/2} \tag{12}$$

This formula makes it possible to determine a surface of the displacement body along the body, except at a small vicinity of the

transom, and this surface will be included in S_m in equations (8) and (9), and for the calculations of pressure and form resistance. However, formula (12) is not applicable to the viscous wake, and another rule is necessary to prolong the equivalent body in the hull wake region.

For a transom stern, the near wake area is a viscous separation zone. Because the flow separation line on the transom are known, Kirchhoff's idea to consider the separation zone as a constant pressure zone in inviscid fluid is good enough, and a boundary of this zone can be included in prolongation of the equivalent displacement body. Currently, it is not difficult to solve a numerically nonlinear axisymmetric problem for finding such an isobaric boundary. Numerical aspects of the iterative technique, which was used in these calculations, were recently described by Amromin (2002), with demonstration of convergence of this technique.

An issue is to determine the values of the base pressure coefficient in inviscid flow C_{PT} and boundary radius in an auxiliary flow $R(x)$. However, a satisfactory determination of these characteristics can be performed with an auxiliary estimation of characteristics of the far wake (Gogish & Stepanov 1982).

In the far wake the following tendencies take place: $\delta^* \to \delta^{**}$ and $R(x) = \delta^* \to [C_V S_w/\pi]^{1/2}$. This formula takes into account that the far wake cross-sections tend to be circular for any body (Birkhoff & Sarantonello 1957). Coefficient C_V includes contributions to the drag from both friction and all pressure perturbations except the effect of the waves; but C_V is unknown while C_{PT} is unknown. The total force balance is:

$$\pi {\delta^*_\infty}^2 S_W + S_T C_{PT} = S_W C_f - 2\int_{S_S}\int N_x u U ds \qquad (13)$$

Here u is a perturbation of U due to the inverse boundary layer influence, the subscript "T" relates to transom, and the subscript "∞" relates to the far wake. Let us suppose that the terms in the right-hand side of equation (13) insignificantly depend on the wake shape. Then two unknown terms are in the left-hand side only. Because $\pi {\delta^*_\infty}^2 = \theta_\infty^*$, the equation (10) can be used to link U (and C_P) with δ^*_∞. For wakes, the right-hand part of equation (10) is zero, and the equation can be simplified:

$$\frac{d(U^2\theta^{**})}{dx} = -\theta^* U \frac{dU}{dx}, \qquad (14)$$

and integrated upstream from the downstream cross-section of wake:

$$U^2\theta^{**}\Big|_{X=X_S}^{X=\infty} = \frac{1}{2}\int_1^{(1+\delta)^2} \theta^* d\zeta \qquad (15)$$

Here $\varepsilon = U_T - 1 \ll 1$, $U_T = (1 - C_{PT})^{1/2}$. Smallness of ε allows the estimation of the integral in the right-hand side of equation (15) with an approximate formula. For the presented computations, this equation is reduced to the following linear equation for ε:

$$\varepsilon(2\theta_T^{**} + \theta_T^* - C_f S_w - C_I) = C_f S_w + C_I - \theta_T^{**} \qquad (16)$$

Here C_I is the integral from equation (13), the friction coefficient C_F is determined with the usual International Towing Tank Conference (ITTC) 1957 formula, and a jump of the value of θ^* at the transom is taken into account. When the transom pressure is found from equation (16), whole equivalent displacement body can be designed and u-distribution corrected. Thus, the form resistance can be refined through an iteration process. The above suggested integration procedure reduces a computation error because $H^* - 1 > 1$, and $\varepsilon \ll 1$ for this type of flow.

There is also a formal aspect related to calculation of u-distribution over the body with a transom. It is necessary to supply a real body contour by some artificial sharp trailing edge. Although the whole pressure and velocity distribution will be in agreement with the D'Alembert paradox, the u-distribution over the side hull surfaces itself gives a correction that contributes to the form resistance. It is possible to calculate u with the formula (9) accepting $Q = 2U\, d\delta^*/dx$.

Thus, the transom contributes $C_T = 2\varepsilon S_T/S_W$ to the residuary drag coefficient. However, a separation zone behind the transom has an influence on pressure distribution over the whole stern, and this inverse influence affects trim and the transom area. Further, the solution of equations (10) and (11) is used in a reinterpolation of the coordinates of submerged parts of the hull, and these corrected coordinates are used in calculation of wave resistance.

Generally, equation (16) can have both positive and negative solutions, and then the above definition of C_T could give a negative drag. That should be excluded, and the calculations are provided for the case $\varepsilon = 0$ that corresponds to the dry transom.

Comparison of measured data and the above-described calculations with the account of the viscous-inviscid interaction is plotted in Fig. 9. There is a clear improvement of calculated trim in this method, and the calculated trim values can be considered as satisfactory. F9

RANS computational verification of MQLT viscous drag trends

Due to the many viscosity-related assumptions of MQLT, however, the authors thought it prudent to perform an independent assessment of these trends by advanced computational tools. Two effects, in particular, require verification: the predicted reduction in residuary resistance with Reynolds number and the decrease of trim-induced drag with Reynolds number. Such an assessment requires the accurate resolution of complex three-dimensional boundary layers at high Reynolds number and must therefore be based on a solution of the RANS equations. Two RANS packages

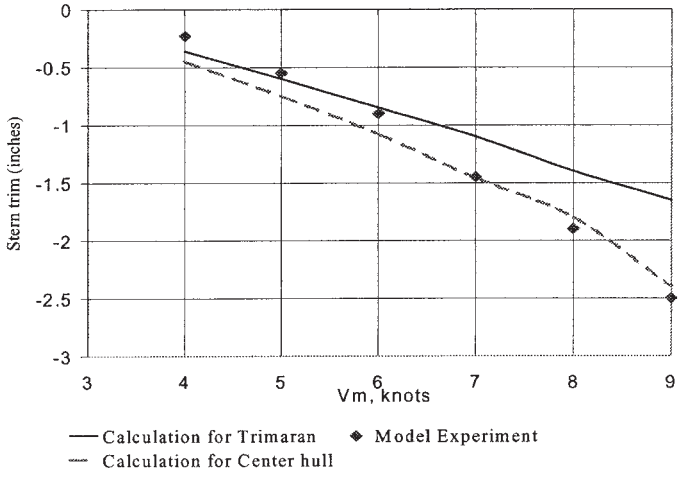

Fig. 9 Measured and calculated trim of stern for the Model B and its calculated trim for its center hull

were chosen for performing the required simulations: Applied Fluid Technologies Incompressible Navier-Stokes (AFTINS) and OVERFLOW. AFTINS is a finite-analytic code developed specifically for the analysis of marine vehicles. It utilizes time-accurate discretization and a k-ε turbulence model. These codes have been validated over a wide range of applications with description of the algorithm convergence (by Chen & Korpus 1993 and by Korpus & Falzarano 1997).

OVERFLOW is a NASA code offering a wide range of discretization and solution options. It solves the compressible form of the RANS equations and must therefore rely on preconditioning to reach Reynolds numbers required for marine applications. It does, however, provide a diverse choice of turbulence models and can be easily applied over a wide range of Reynolds numbers. OVERFLOW has also been validated on a wide range of practical engineering problems (Benek et al 1985, Jespersen & Levit 1989).

These two codes were selected because both of them permit the use of overset grids. This is a critical advantage for accuracy and efficiency because overset methods allow neighboring grid blocks to be generated without regard to how they intersect. Interblock communication is provided by conservative interpolation, enabling high-quality grids (and therefore more accurate solutions) to be generated in less time and with fewer points.

The calculations of the large high-speed trimaran were provided with its side hulls in their aft position, and with sinkage and trim held fixed at prescribed values. Because the study is intended to identify viscous-related effects missing from MQLT, free-surface shape was held fixed for all RANS runs. Full-scale ship speed was assumed to be 50 knots full scale, and the transom was assumed dry at all times.

Computational meshes were developed using NASA's HYPGEN and SURGRD suite of hyperbolic grid-generation tools. The hull near-field regions are each resolved with four body-fitted, curvilinear blocks. Two Cartesian far field blocks surround these, and carry the outer boundaries to two body lengths upstream and athwartships, and four body lengths downstream. Total grid size is approximately 1.1 million points. Initial wall spacing (prior to grid-dependency studies) was set to 10^{-8} of center hull length.

OVERFLOW was run in its "incompressible preconditioning" mode, and third-order upwind differencing was used for all flow variables. The Spalart-Allmaras one-equation turbulence model (Spalart and Allmaras 1992, Edwards et al 2001) was found to provide a good compromise between accuracy and robustness, and was used for all OVERFLOW results presented herein. Because of this robustness, OVERFLOW was used for all simulations at full-scale Reynolds number.

Three separate run series were performed: a near-wall grid-dependency series; a Reynolds number series; and a trim series. The grid-dependency study consists of five values of near-wall grid spacing ($y = 0.1$, 0.5, 1.0, 5.0, and 10.0) and was used to identify optimum grid resolution across the range of Reynolds numbers. The series were completed at two Reynolds numbers; one typical of model scale (2×10^7), and one typical of full scale (2×10^9). The results show that for the moderate near-wall spacing ($y = 0.5$, 1.0, and 5.0), drag trends differ between the various geometries by less than 2% of total drag. A total of 10 RANS runs was made and resulted in a spacing of $y = 1.0$ being selected for the remaining investigations.

Once an optimal grid resolution was found, a second run series was initiated to investigate the effect of Reynolds number. Three Reynolds numbers (2×10^7, 2×10^8, and 2×10^9) were used, and the grid resolution changed each time to maintain near-wall spacing at $y = 1.0$. A third run series investigated the effect of trim on drag and trim moment. Stern trims of 0.0, 0.2, 0.4, 0.6, and 0.8 deg were used, and the run series repeated at each of the three Reynolds numbers. The second and third run series together constitute 15 RANS runs.

Validation of the RANS codes and problem setup was made by comparing computational predictions to laser light sheet measurements made at the David Taylor Model Basin. Because the light sheet tests were conducted on a Model B with side hulls mounted in their forward position, new computational grids were first developed. Great care was exercised during this process to ensure the new grids were geosyms of their aft side hull counterparts. The comparison consists of athwartships boundary layer cuts at $x/L = 0.5$ for the 0.6 deg aft trim case. The RANS prediction from AFTINS and the light sheet counterpart comparison is described in Allison et al (2000) and showed that OVERFLOW results are only slightly different than the AFTINS predictions. AU5

Although a lot can be learned from such results, the main objective was integrating the RANS-predicted normal pressure and skin friction over each of the hull surfaces. Because only Reynolds number–dependent effects on the hull surfaces are under investigation, transom wave drag was first subtracted using the following technique. Each grid was run through the RANS code a second time, but with all viscous derivatives removed and no-slip boundary conditions negated. The resulting Euler solutions give zero viscous drag and would yield zero form drag for a closed surface. Because the hulls are not closed surfaces, however, the pressure integral gives the wave drag associated with maintaining a dry transom. The difference between RANS and Euler pressure integrals is accepted as form drag.

The resulting drag components are defined according to the formulae:

$$C_{df} = 2\int\int \bar{i} \cdot (\bar{\bar{\tau}} \circ \bar{N}) ds/\rho V_s^2 S$$

$$C_{dp} = \int\int \bar{i} \cdot \bar{N} (P_{RANS} - P_{EULER}) ds/\rho V_s^2 S$$

$$C_{dv} = C_{df} + C_{dp}$$

$$C_{mv} = 2\int\int \bar{j} \cdot \bar{R} \times (\bar{\bar{\tau}} \circ \bar{N}) ds/\rho V_s^2 SL + 2\int\int \bar{j} \cdot \bar{R} \times \bar{N} (P_{RANS} - P_{EULER}) ds/\rho V_s^2 SL$$

Here P is the normal static pressure, $\bar{i}$ and $\bar{j}$ are unit vectors in the drag and pitch directions, respectively; $\bar{\bar{\tau}}$ is the anisotropic portion of the fluid stress tensor, and the symbol "$\cdot$" means the product of tensor and vector. $\bar{R}$ is a position vector from the longitudinal center of flotation to an arbitrary point on its wetted surface. Although this breakdown of drag is different from traditional naval architecture, a form factor can be derived from these results by taking the ratio of friction plus form drag to that of a flat plate reference line (e.g., ITTC line).

Figure 10 shows viscous drag results from the second and third run series plotted versus Reynolds number. One curve is included for each stern trim, and the ITTC friction line has been added for reference. As expected, drag increases with stern trim, and decreases with Reynolds number. The rate of decrease with Reynolds F10

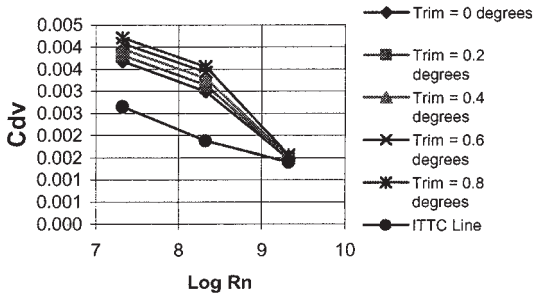

Fig. 10 Viscous drag versus Reynolds number. ITTC = International Towing Tank Conference

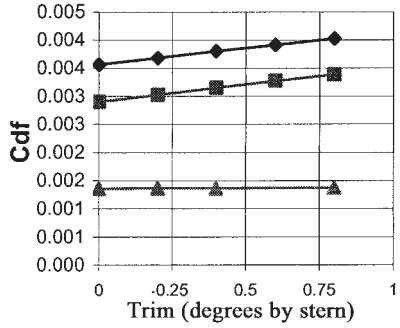

Fig. 11 Skin friction drag versus trim. Rhombs relate to Rn = 10^7, squares relate to Rn = 10^8, triangles relate to Rn = 10^9

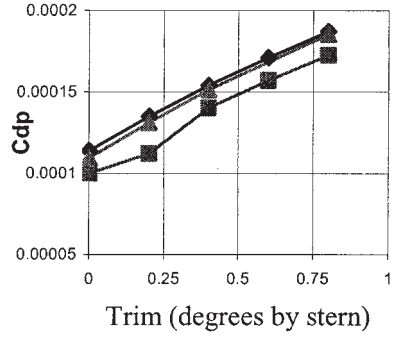

Fig. 12 Pressure integral drag versus trim. Rhombs relate to Rn = 10^7, squares relate to Rn = 10^8, triangles relates to Rn = 10^9

number, however, is significantly different from that predicted by the ITTC line. The curves remain approximately parallel up until a Reynolds number of 10^8, after which RANS begins a steeper drop in drag. At full-scale Reynolds numbers, RANS-predicted drag is only 5% to 10% above the ITTC line.

F11 F12 F13 Figures 11, 12, and 13 show the skin friction, form drag, and total drag as function of trim. Both components of drag increase with trim as expected, with form drag almost doubling over the range investigated. Figure 14 also indicates that for a given trim, form drag is essentially independent of Reynolds number, and all pressure integral drag components lie within 1% total drag of each other. Skin friction (in Fig. 11) shows the dependence on Reynolds number that is expected but highlights a decreasing dependence on trim as Reynolds number increases.

Finally, Fig. 14 shows curves of nondimensional viscous trim moment versus trim, one curve for each Reynolds number. Contrary to MQLT, it indicates that viscous trim moment is not a particularly strong function of Reynolds number. This discrepancy is thought to be a by-product of having frozen the free surface shape in the RANS simulations. This has the effect of removing any feedback from viscous-related free-surface changes back onto the trim moment itself. In other words, viscous boundary layer effects do not change the trim moment, but the effect of the boundary layers on the free surface does. F14

Nevertheless, these results demonstrate that RANS simulations verify many of the MQLT hypotheses outlined elsewhere in this paper. In particular, total viscous (i.e., nonwave) drag decreases with Reynolds number faster than predicted by flat plate friction lines, and most of this decrease is due to skin friction reduction rather than form drag reduction. Equally important is that model test–derived form factors can overpredict full-scale drag, thus verifying the need for negative values of the correlation coefficient (SCC) in scaling model test residual resistance for high-speed transom hulls. A final observation from MQLT-RANS results is that skin friction increases with trim more gradually as Reynolds number increases.

Comparison of calculated and measured residuary drag

The modified QLT (MQLT) calculations of residuary drag of the trimaran take into account the following drag components:

- Wave resistance at its dynamic trim and sinkage
- Form resistance (including the transom contribution)
- Variation of friction due to the dynamic variations of the wetted surface.

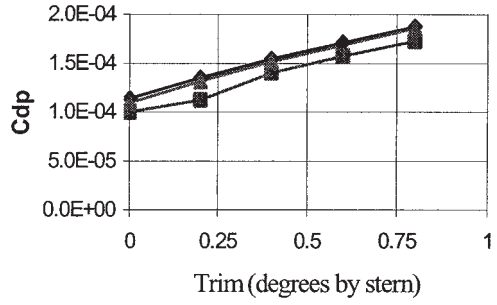

Fig. 13 Total viscous drag versus trim. Rhombs relate to Rn = 10^7, squares relate to Rn = 10^8, triangles relate to Rn = 10^9

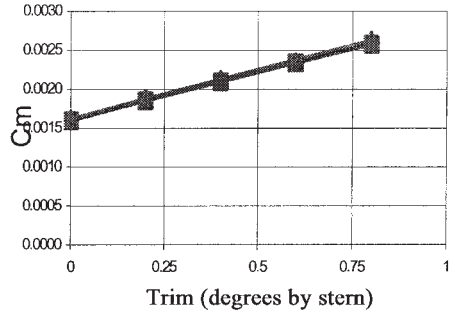

Fig. 14 Trim coefficient versus trim. Rhombs relate to Rn = 10^7, squares relate to Rn = 10^8, triangles relate to Rn = 10^9

The MQLT calculations are compared with measured data for Model A at two locations of side hulls (in Figs. 15 and 16). For the forward position of side hulls, the distance between their sterns and the center hull stern was 3 m (about a half of the center hull model length). For the aft position, the sterns of the center hull and the side hulls are at the same line.

Towing tank tests of the Model B were carried out only for the forward position with the free pitch. The comparison of measured and calculated C_R for this model is shown in Fig. 17.

A remarkable difference in the maximal C_R values and the forms of dependencies C_R(Fn) for two models cannot be explained only by the changes in the shape of the center hull stern. The comparison of residuary drag coefficient for isolated center hulls of two models in Fig. 18 is a proof of this statement. The higher drag of the Model A center hull (with the larger transom without a slope) in the high-speed range is caused by a double effect: first, an increase of S_T results in the C_T increase; second, submergence of the blunter stern leads to a C_R increase.

These results correspond to the conclusion made by the 22nd ITTC, which pointed out that the use of a form factor for high-speed ships in a traditional manner (proposed by 1978 powering performance procedure) is not reliable and sufficient. If, as it is in our case, a high-speed vessel employs transom stern, leading to a confused flow aft of the transom at low speed and wetted surface generally changes with the speed, resulting in a change in true form factor with speed.

However, returning to the trimaran and comparing forces (not dimensionless coefficients related to wetted surfaces that are very different for trimaran and its center hull), one can find that the difference between drag for two models is two times higher than the difference for their center hulls. This effect is mainly caused by a difference in the submergence of side hulls. Their aft location leads to the increase of the wetted surface (and corresponding increase of the friction drag) and to the increase of the side hulls transoms drag.

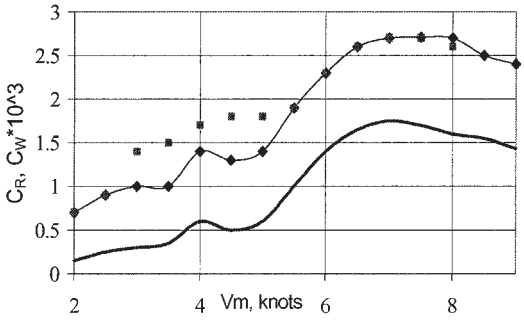

Fig. 15 Comparison of calculations and measurements of C_R for Model A with free pitch at the aft position of side hulls. Squares show experimental C_R, computed C_R is shown by solid line with rhombs, computed C_W is plotted by solid line

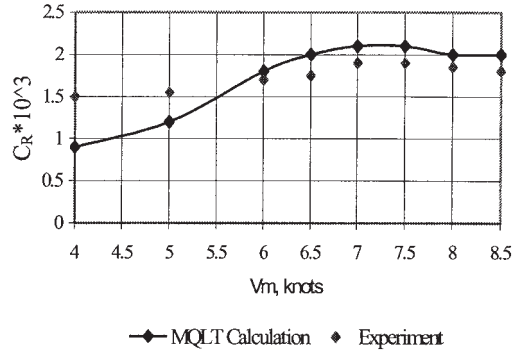

Fig. 16 Comparison of calculations and measurements of C_R for Model A with free pitch at the forward position of side hulls

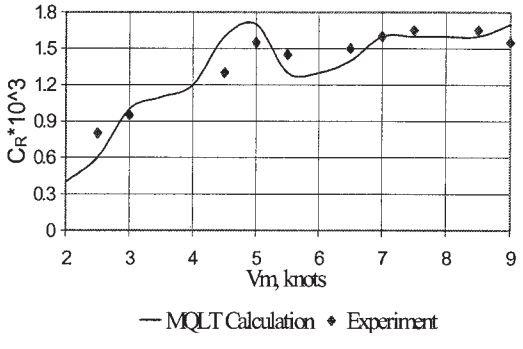

Fig. 17 Measured (squares) and calculated with modified quasi-linear theory (MQLT; solid line) C_R for Model B

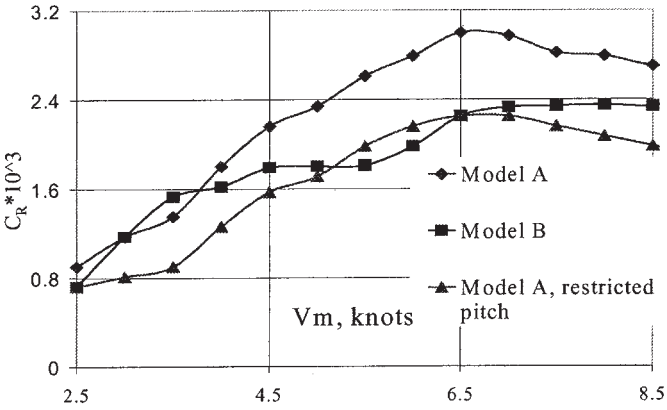

Fig. 18 Calculated C_R of center hulls with free pitch (for Model A and Model B) and restricted zero pitch for Model A

Scale effect on trimaran residuary drag: scale correlation coefficient

The described model tests were assigned for a trimaran with the center hull length of 313 m. It is reasonable to expect scale effects on C_R. MQLT allows an estimate of the scale factor that can be introduced in the ship resistance prediction in the terms of the scale correlation coefficient (SCC).

According to the MQLT calculations, the scale effect on trimaran residuary drag is mainly associated with Re influence on the stern trim (one can see an example of the computed scale effect on trim in Fig. 19; relative trim is the ratio of 100 stern submergences to $L/2$ there). It is necessary to mention that the trim slow decrease at $\sim$0.5 is in perfect accordance with the recent full-scale observation of a 78-m fast catamaran (Armstrong 1999).

Why does an increase in the Reynolds number lead to a trim drop? The transom pressure depends on the boundary layer

thickness (as it takes place for the pressure behind obstacles within boundary layer) and affects the pressure distribution in the vicinity of transom. In the physical process of originating and further development of the running trim, this vicinity is the most important part of the hull.

The MQLT calculations for model and full scale of two hull forms (Models A and B) are shown in Figs. 20 and 21. One can see in these figures that difference in C_R values (SCC to be defined as C_R ship $-$ C_R model) can be very different for different stern shapes and mutual position of center hull and side hulls. The calculations show SCC can vary from -0.0005 (for Model B) to -0.0001 (for Model A).

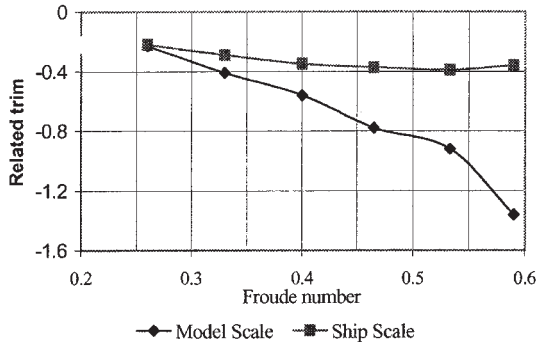

Fig. 19 Modified quasi-linear theory calculation of scale effect on trim at stern of the Model B

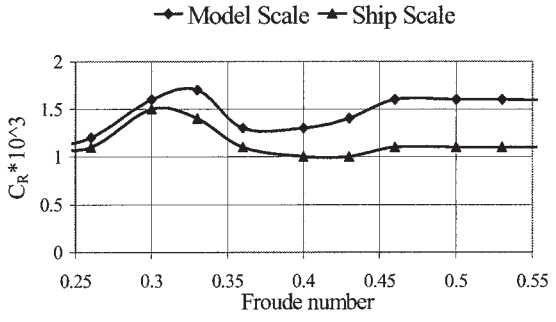

Fig. 20 Modified quasi-linear theory calculations of residual resistance at model and ship scales for Model B

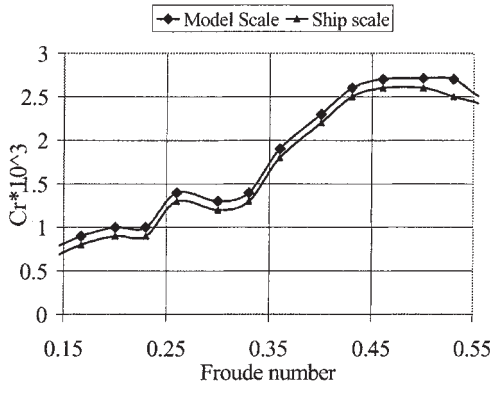

Fig. 21 Modified quasi-linear theory calculations of residual resistance at model and ship scales for Model A

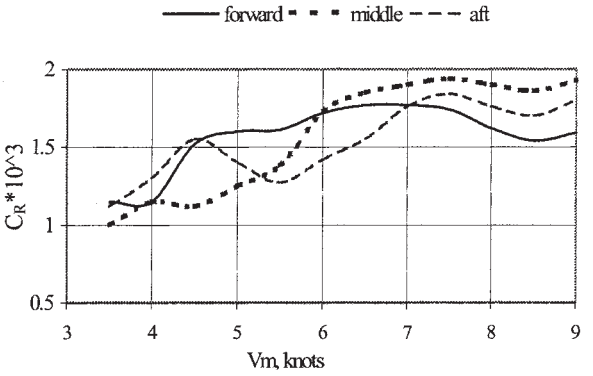

Fig. 22 Calculated "model scale" residuary drag coefficient for Model B with different longitudinal position of side hulls

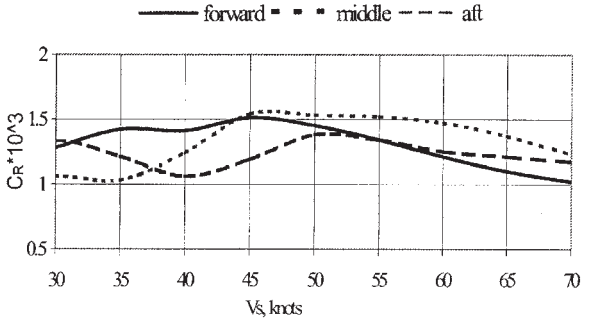

Fig. 23 Calculated "ship scale" residuary drag coefficient for the trimaran ship with different longitudinal position of the side hulls

A negative correlation coefficient for large monohull ships has been observed earlier (Karafiath 1997). For a large multihull, this correlation value can be also high (Armstrong 1999). A surprise is the significant difference in the SCC for trimarans of the same length, but a good agreement of computation with model test data urges us to trust this theoretical result.

Here is the right place to consider the question of whether there is a different scale effect on the position of the side hulls. The comparative MQLT calculations are shown in Figs. 22 and 23.

Taking into account that the scale ratio about of 1:50 results in the speed ratio 1:7 for the same values of Fn, one can compare curves at Figs. 22 and 23. There is a certain similarity of model-related and full-scale-related dependencies, but the values of correlation coefficients (SCC) clearly depend on side hull positions.

Conclusions

For trimaran shape optimization, a wave resistance minimization was traditionally the major driving force. Contemporary numerical methods for C_W estimation work satisfactorily for monohulls and SWATH at moderate Fn, and these methods have seemed to be a sufficient basis for C_R prediction because the viscous part of C_R can usually be successfully extrapolated from small Fn values to its moderate and even high values. However, comparisons of experimental and computed data for models of the large high-speed trimarans have shown a large difference between measured and computed C_R. This difference clearly indicates that

results of towing tests for slender hulls with large transoms at small values of Fn are not informative for prediction of full-scale ship performances at these values. The difference between measured and computed C_R clearly depends on Fn, thus proving the 22nd ITTC statement about form factor dependence on speed for high-speed vessels. It is necessary to understand the situation and be able to correctly extrapolate the model test results to full-scale condition. Accordingly, a novel problem on viscous-inviscid interaction must be considered.

A concept of solving this problem is described in this paper. The investigation based on this concept (MQLT) showed that the unusually high Froude-dependent difference between C_R and C_W of high-speed trimarans is associated mostly with their trim. This difference includes mainly an increase of friction (caused by a rise of the wetted surface) and of transom drag (caused by an increase of its area at high Fn values). Consequently, there is a part of viscous drag that directly depends on Fn. On the other hand, for any Fn, trim significantly depends on the transom pressure that can be found from computations of hull boundary layer and viscous separation past the transom (and depends on Rn.)

As was shown by comparison with results of towing tests, MQLT allows a satisfactory prediction of trimaran residuary drag. Thus, the MQLT implementation for approximate determination of full-scale drag of trimarans and their correlation coefficient looks reasonable. This correlation coefficient, SCC being negative in the range from -0.0005 to -0.0001, as it is estimated here for the slender high-speed trimaran hull forms, should be added to the model residual drag in the ship power prediction procedure. One of the important findings is the substantial dependency of this correlation coefficient on the relative location of trimaran hulls.

The actual numerical realization of MQLT combines previously validated numerical techniques, includes many simplifications, and could be partially replaced by more advanced methods. The certain step in this direction is the described analysis of viscous drag with RANS codes. Currently, these codes were used rather for some kind of validation for MQLT; the future applications may be much wider. Nevertheless, a possibility of estimating the residuary drag of slender hulls by using simplified numerical methods will be still important, especially for the multivariant analysis in the hull development optimization problem of high-speed ships.

Acknowledgment

This paper became possible with funding and support from the U.S. Center for Commercial Deployment of Transportation Technologies. Acknowledgment is due to Kvaerner Masa Marine, Inc. (KMM), Annapolis, Maryland, USA, for allowing the use of the model test data to validate the theories and calculations presented in this paper and for managing the major projects during the time of this work. Special thanks are due to Susan Parker and John Avis of KMM for their help and encouragement.

AU7

References

ALLISON, J., BECNEL, A., MIZINE, I., AND PURNELL, J. 2001. 80-100 MW "unified propulsion package" for the very high speed sealift trimaran (VHSST) design application, *Proceedings*, Waterjet Propulsion III Conference, Sweden.

AMROMIN, E. L. 2002 Scale effect of cavitation inception on a 2D Eppler hydrofoil, *Journal of Fluids Engineering*, **124**, 186–193.

AMROMIN, E. L., IVANOV, A. N., MIZINE, I. O., AND TIMOSHIN, Y. S. 1984 On the influence of non-linearity of boundary conditions at hull and water surface in the problem of a ships wave resistance, *Proceedings*, XV Symposium on Naval Hydrodynamics, Hamburg, Germany.

AMROMIN, E. L., LORDKIPANIDZE, A. N., AND TIMOSHIN, Y. S. 1993 A new interpretation of linear theory in the calculation of ship wave resistance, JOURNAL OF SHIP RESEARCH, **37**, 7–12.

AMROMIN, E. L., MIZINE, I. O., PASHIN, V. M., AND TIMOSHIN, Y. S. 1983 Minimum resistance hull form problem and methods of improving real ship lines, *Proceedings*, International Symposium on Ship Hydrodynamics Energy Saving, El Pardo.

ANDO, J., SHIOTA, H., KATAOKA, K., AND MAKATAOKA, K. 1990 Free surface effect on propulsion performance of a ship, *Transactions of the West-Japanese Society of Naval Architects*, **79**.

ARMSTRONG, N. A. 1999 From model scale to full size—toward an understanding of the scaling of resistance of high-speed craft, *Proceedings*, FAST-99, Seattle, 781–787.

AVIS, J., MIZINE, I. O., AND PARKER, S. 1999 Development of high speed sealift ships, *Proceedings*, CIMarE High-Speed Vessel Conference, Victoria, BC, Canada.

BENEK, J., BUNING, P., AND STEGER, J. 1985. A three-dimensional CHIMERA grid embedding technique, AIAA 85-1523-C.

BIRKHOFF, G., AND SARANTONELLO, E. 1957 *Jets, Wakes and Cavities*, Academic Press.

CHEN, H.-C., AND KORPUS, R. 1993 A multi-block finite-analytic Reynolds-averaged Navier-Stokes method for 3D incompressible flows, *Transactions of ASME Summer Fluids Engineering Conference*, Washington, DC.

EDWARDS, J. R, ROY, C. I, BLOTTNER, F. G., AND HASSAN, H. A. 2001 Development of a one-equation transition/turbulence model, *AIAA Journal*, **39**, 1691–1698.

GRANVILLE, P. S. 1974 A modified Froude method for determining full-scale resistance of surface ships from towed models, JOURNAL OF SHIP RESEARCH, **18**, 4.

GOGISH, L. V., AND STEPANOV, G. Y. 1982 Turbulent separating flows, *Fluids Dynamics*, **17**, 181–197.

HAVELOCK, T. H. 1934 The calculation of wave resistance, *Proceedings*, Royal Institution of Naval Architects, London.

HUANG, D. L., AND CAI, Y. J. 1991 An optimization method for hull form design of SWATH ships, *International Shipbuilding Progress*, **38**, 193–205.

INUI, T. 1957 Study on wave-making resistance of ships, *Transactions of SNEJ*, **2**.

ITTC-22. 2001 *Final Report and Recommendations of the Specialist Committee on Model Test of High Speed Marine Vehicles*, International Towing Tank Conference.

JESPERSEN, D., AND LEVIT, C. 1989 A computational fluid dynamics algorithm on a massively parallel computer, *International Journal of Supercomputer Applications*, **3**, 4, 9–27.

KARAFIATH, G. 1997 US Navy ship-model powering correlation and propeller RPM prediction, *Proceedings*, SNAME Propeller-Shafting Conference, Virginia Beach, VA.

KENNELL, C. 1998 Design trends in high speed transport, *Marine Technology*, **35**, 3.

KORPUS, R., AND FALZARANO, J. 1997 Prediction of viscous ship roll damping by unsteady Navier-Stokes techniques, *Journal of Offshore Mechanics and Arctic Engineering*, **119**, 2, 108–113.

LALLI, F., CAMPANA, E., AND BULGARELLI, U. 1992 Ship wave computation, *Proceedings*, International Workshop on Water Wave Floating Bodies, Val de Rueil, France.

LARSSON, L., REGNSTROM, B., BROBERG, L., LI, D.-Q., AND JANSON, C.-E. 1998 Failures, fantasies and feats in the theoretical/numerical prediction of ship performances, *Proceedings*, 22nd Symposium on Naval Hydrodynamics, Washington, DC.

MIZINE, I. O., AND AMROMIN, E. L. 1999 Large high-speed trimaran: optimization concept, Proceedings, FAST-99, Seattle, WA.

MIZINE, I. O., AND THORPE, R. 2000 High speed slender monohull-trimaran optimized chain of efficiency, *Proceedings*, IMAM-2000, Naples, Italy.

NI, S. Y., KIM, K. J., XIA, F., AND LARSSON, L. 1989 High-order method for calculating free surface potential flows with linear surface boundary conditions, *Proceedings*, International Symposium on Ship Resistance, Shanghai, People's Republic of China.

ORIHARA, H., AND MIYATA, H. 2000 Numerical simulation method for flow about a semi-planing boat with a transom stern, JOURNAL OF SHIP RESEARCH, **44**, 170–185.

SALVESEN, N., AND VON KERCZEK, C. 1976 Comparison of numerical and perturbation solution of two-dimensional nonlinear water-wave problems, JOURNAL OF SHIP RESEARCH, **19**, 160–170.

SPALART, P., AND ALLMARAS, A. 1992 A one-equation turbulence model for aerodynamic flows, *Proceedings*, AIAA 29th Aerospace Sciences Meeting, Reno, NV, AIAA-92-0439.

TODD, F. H. 1953 Some further experiments on single-screw merchant ship forms—series 60, *Transactions of the Society of Naval Architects and Marine Engineers*, **61**.

YANG, C., NOBLESSE, F., LOHNER, R., AND HENDRIX, D. 2000 *Practical CFD Applications to Design of a Wave Cancellation Multihull Ship*, Society of Naval Architects and Marine Engineers, Jersey City, NJ.

AUTHOR'S QUERY

1. <<1>>AU: Please add city and state of Science Applications International Corporation.<</1>>
2. <<2>>AU: Please check spelling of von Kerzeck. It is spelled von Kerczek in the reference list.<</2>>
3. <<3>>AU: Do you mean the "customary" path?<</3>>
4. <<4>>AU: Is the slash after the superscript 1 correct?: "$(x\ L/\mathrm{Rn})^{1/}$"<</4>>
5. <<5>>AU: Do you mean Allison et al (2001)? If not, please add Allison et al (2000) to the reference list.<</5>>
6. <<6>>AU: Are there words missing in the following sentence?: "If, as it is in our case, a high-speed vessel employs transom stern, leading to a confused flow aft of the transom at low speed and wetted surface generally changes with the speed, resulting in a change in true form factor with speed."<</6>>
7. <<7>>AU: Reference queries:
Please add months of conferences to Allison, Amromin et al 1983 and 1984, Armstrong, Avis, Havelock, Karafiath, Larsson, Lalli, Mizine 1999 and 2000, Ni, and Spalart.
Ando: please add page numbers.
If Benek is a paper presented at a conference, please add name, location and month of conference.
Birkhoff: please add city of publication.
Chen: Are volume and page numbers available?
Inui: please add page numbers.<</7>>